Paper No. 18-01782

Effects of Freeze-Thaw Cycles and Anti-Stripping Agents on Hot Mix Asphalt Dynamic Modulus

Adrian Ricardo Archilla, Ph.D.[1]
Associate Professor, University of Hawaii at Manoa,
2540 Dole Street, Holmes Hall 383
Honolulu, HI 96822
Phone: (808) 956-3348, fax (808) 956-5014, email: archilla@hawaii.edu

Jose Corrales-Azofeifa, Ph.D.
Jas. W. Glover, Ltd., P.O. Box 579,
Honolulu, HI 96809, USA,
Phone: (808) 591-8977, fax (808) 591-8978, email: josec@gloverltd.com

Fabiola Miranda-Argüello
Transportation Infrastructure Program
National Laboratory of Materials and Structural Models (LanammeUCR)
University of Costa Rica, P.O.Box 11501-2060, UCR, San José, Costa Rica
Phone: +(506) 2511-2539, fax: + (506) 207-4442, email: fabiola.miranda@ucr.ac.cr

Luis Loria-Salazar, Ph.D.
Transportation Infrastructure Program Director
National Laboratory of Materials and Structural Models (LanammeUCR)
University of Costa Rica, P.O.Box 11501-2060, UCR, San José, Costa Rica
Tel: +(506) 2511-4122, fax: + (506) 207-4442, email: luis.loriasalazar@ucr.ac.cr

Acknowledgements
The financial support of the State of Hawaii Department of Transportation (HDOT) – Airports Division (Honolulu International Airport) and the University Transportation Center for Highway Pavement Preservation is greatly appreciated and acknowledged. The contents of this paper reflect the view of the writers, who are responsible for the facts and accuracy of the data presented herein. The contents do not necessarily reflect the official views or policies of the State of Hawaii Department of Transportation or the Federal Highway Administration. The contents contained herein do not constitute a standard, specification, or regulation.

The first two authors are grateful to Mr. Gaudencio Lopez, P.E. and Oahu District Engineer, Honolulu International Airport for his support.

Word Count: Text: 1749

[1] Corresponding Author

INTRODUCTION

This study shows how the number of freeze-thaw cycles (FTC) and use of anti-stripping agents were incorporated in a model for Hot Mix Asphalt (HMA) dynamic modulus, |E*|, and discusses the engineering implications related to these two factors. The model was estimated using the statistical approaches of joint estimation and mixed-effects with 6821 observations from 265 specimens in 3 different datasets (*1*). Two datasets were collected at the University of Hawaii (UH) pavement laboratory and the third one at the National Laboratory of Materials and Structural Models of the University of Costa Rica, LanammeUCR. The datasets contain variables in common such as air voids, binder content, and gradation and variables not available in all datasets such as confinement level, FTC, anti-stripping agents, and fibers.

Moisture Damage

Moisture damage is a result of a loss of adhesion between asphalt and aggregates or a loss of cohesion and stiffness of the binder or the mastic (2-*8*).

To induce moisture damage, many standards rely on conditioning samples in water baths before or during testing. Epps et al. (*9*) recommended the use of a freeze-thaw cycle in AASHTO T283. Multiple conditioning cycles have also been used for a more accurate simulation of field performance (*10*).

Several tests are available to evaluate moisture susceptibility of asphalt mixtures but, at present, AASHTO T283 is the most commonly used (*11,12*). Several agencies have reported difficulties with this test for evaluating field conditions (*11*). Some studies (*10*,*11*) have suggested the use of |E*| to measure the susceptibility of asphalt mixtures to moisture damage.

Anti-stripping Agents

Anti-stripping agents are used to counteract moisture damage effects. Hydrated lime is the most common anti-stripping additive used with widely reported benefits (*4*). It improves the binder-aggregate adhesion (*6*) and decreases the compatibility between binder and water (*13*). The other liquid anti-strip used in this study is a chemical compound that contains amines (*14*) and works by reducing the surface tension between aggregates and binder, therefore promoting an increased adhesion of the two materials.

Master Curve

|E*| at any temperature and frequency is computed from a master curve, which is an interpolation model from a set of measured values. Master curves have two main components. The first is typically a sigmoidal function relating |E*| to a reduced frequency f_r at a reference temperature T_r. For convenience, the typical sigmoidal curve was modified as:

$$\log(|E^*|) = \rho - \frac{\alpha \cdot \alpha_{cf}}{1+e^{-\left(\beta+\gamma\left(log(1/f_r)\right)\right)}} \quad (1)$$

where the parameters α, β, and γ are the same as in the typical sigmoidal curve. Parameter ρ represents the maximum of the log(|E*|) (the typical sigmoidal curve also uses a parameter δ representing the minimum of the log(|E*|); the relationship between these parameters is $\rho = \delta + \alpha$). An additional parameter α_{cf} was introduced to account for the effects of confinement (not discussed here). Without confinement ($\alpha_{cf} = 1$), Eq. (1) is simply a different parametrization of the typical sigmoidal curve but with some statistical and engineering advantages (*1*).

The second component of the master curve defines a shift factor $a(T) = \frac{f_r}{f}$ as a function of temperature, *T*:

$$\log\big(a(T)\big) = \mathrm{A}\,T^2 + B\,T + C \tag{2}$$

where *A*, *B*, and *C* are model parameters.

METHODOLOGY

Only the dataset from Costa Rica contains information on the effects of FTC and antistripping agents. The two datasets from Hawaii (herein referred as UHO and UHN), contain 5404 data points for 122 specimens with 12.5-mm Nominal Maximum Aggregate Size (NMAS) gradations prepared with different binders, with and without polyolefin/aramid fibers, different confinement and air voids levels, and combinations of these factors. Further details are given in references (*1,10*).

The Costa Rican dataset, herein referred to as CR, was collected by LanammeUCR. Twelve Superpave mix designs were performed with igneous aggregates and two different aggregate gradations with 9.5-mm and 12.5-mm NMAS. A total of 143 specimens with 7% target air voids were mixed and compacted producing 1417 points. A virgin PG70-22 and a polymer modified PG76-22 were used. Some specimens were treated with a commercial liquid anti-stripping agent at a rate of 0.5% by total weight of binder, and others with hydrated lime at a rate of 1% by total weight of aggregate.

Table 1 shows the variables used in the final model specification. The three datasets help to identify the effects of several variables in common (*f*, *T*, μs, V_{beff}, *AV*, *R4*, and *P200*) but some of the variables can only be identified from a single dataset. Specifically, the effects of FTC and anti-stripping agents can only be identified from the CR dataset. Joint estimation is used to take advantage of the complementary characteristics of the datasets (*15, 16*). Likewise, non-linear mixed effects (NLME) are used to account for the correlation between observations within a specimen due to unobserved factors (*17*).

Model Specification

The complete model specification includes the 20 variables defined in Table 1. The following paragraphs concentrate on the elements of the model related to FTC and anti-stripping agents. For details about the functional forms of other parts of the model see reference (*1*).

Parameter ρ was modeled with three multiplicative terms:

$$\rho = \bar{\rho} \cdot \rho_a \cdot \rho_m \tag{3}$$

where $\bar{\rho}$ is a function of other variables and corresponds to a situation without FTC and no antistripping agents and where the terms ρ_a and ρ_m account for the effects of anti-stripping agents and moisture damage, respectively,

$$\rho_a = 1 + \rho_{Lime}\, D_{Lime} + \rho_{MB}\, D_{MB} \tag{4}$$

$$\rho_m = 1 + \rho_{D1C}\, D_{D1C} + \rho_{D3C}\, D_{D3C} + \rho_{D6C}\, D_{D6C} \tag{5}$$

where $\rho_{Lime}, \rho_{MB}, \rho_{D1C}, \rho_{D3C}$, and ρ_{D6C} are model parameters.

β and γ were also found to be affected by FTC but not by anti-stripping agents:

$$\beta = \bar{\beta} \cdot \beta_m \tag{6}$$

$$\beta_m = 1 + \beta_{D6C}\, D_{D6C} \tag{7}$$

$$\gamma = \bar{\gamma} \cdot \gamma_m \tag{8}$$

$$\gamma_m = 1 + \gamma_{D1C}\, D_{D1C} + \gamma_{D3C}\, D_{D3C} + \gamma_{D6C}\, D_{D6C} \tag{9}$$

where $\beta_{D6C}, \gamma_{D1C}, \gamma_{D3C}$, and γ_{D6C} are model parameters and $\bar{\beta}$ and $\bar{\gamma}$ are functions of other variables yielding β and γ, respectively, for the situation with no FTC and no antistripping agents.

TABLE 1 Variables used in the final model specification

Variable Type	Variable	Dataset	Values per specimen	Description
Dataset	D_{UHO}	UHO	1	1 if observation belongs to UHO, 0 otherwise
	D_{CR}	CR	1	1 if observation belongs to CR, 0 otherwise
Testing conditions	f	All	Several	Frequency (Hz)
	T	All	Several	Temperature (°C)
	μs	All	Several	Microstrain (strain × 10^6)
	σ_3	UHN, UHO	Several	Confining stress (kPa) (only 0 kPa for CR)
Specimen volumetrics and gradation	V_{beff}	All	1	Effective binder content by volume (%)
	AV	All	1	Air voids (%)
	$R4$	All	1	Percent retained sieve No. 4
	$P200$	All	1	Percent passing sieve No. 200
Binder	$D_{PG76UHN}$	UHN	1	1 if PG76-22 binder (UHN), 0 otherwise
	$D_{PG70UHO}$	UHO	1	1 if PG70-22 binder (UHO), 0 otherwise
	D_{Elv}	UHO	1	1 if PG70-XX binder, 0 otherwise
	D_{PG76CR}	CR	1	1 if PG76-22 binder (CR), 0 otherwise
Freeze-thaw cycles	D_{D1C}	CR	1	1 if 1 FTC, 0 otherwise
	D_{D3C}	CR	1	1 if 3 FTC, 0 otherwise
	D_{D6C}	CR	1	1 if 6 FTC, 0 otherwise
Anti-stripping	D_{Lime}	CR	1	1 if lime, 0 otherwise
	D_{MB}	CR	1	1 if liquid anti-strip, 0 otherwise
Fibers	D_{Fib}	UHN	1	1 if polyolefin/aramid fibers, 0 otherwise

Estimation Results

Table 2 shows the FTC and anti-stripping agents parameter estimation results. Other statistical results are presented in reference (*1*).

Since variables D_{Lime} and D_{MB} do not appear anywhere else in the model, the signs of ρ_{Lime} and ρ_{MB} imply that use of either anti-stripping agent simply raises the whole master curve. However, addition of lime results in a bigger increase than that obtained by adding the liquid anti-strip.

TABLE 2 Parameters of the model included in the ρ factor

Eq. (1) Parameter	Parameter	Parameter Estimate	Standard Error	*t* value	*p* value
ρ	ρ_{Lime}	0.0259	1.55E-03	16.708	<0.0001
	ρ_{MB}	0.0112	1.61E-03	6.956	<0.0001
	ρ_{D1C}	-0.0117	2.07E-03	-5.681	<0.0001
	ρ_{D3C}	-0.0208	2.07E-03	-10.034	<0.0001
	ρ_{D6C}	-0.0228	2.27E-03	-10.043	<0.0001
β	β_{D6C}	-0.0554	0.0127	-4.367	<0.0001
γ	γ_{D1C}	0.0381	0.0116	3.281	0.0010
	γ_{D3C}	0.0386	0.0118	3.263	0.0011
	γ_{D6C}	0.0544	0.0125	4.340	<0.0001

The estimates for ρ_{D1C}, ρ_{D3C} and ρ_{D6C} also have intuitively correct negative signs, since they indicate a monotonic reduction of the maximum of log(|E*|) with any FTC level.

β and γ define the shape of the sigmoid. With a negative β, a negative change (or net increase) in β decreases the values of log(|E*|) across all frequencies. The negative estimate of β_{D6C} (-0.0554) indicates that with 6 FTC the mix becomes less stiff, with all else equal.

A positive change in the value of γ with all the other terms fixed (ρ, α, β) makes the values of log(|E*|) increase (albeit, by a small amount) for f_r greater than 1 and decrease more substantially for f_r below 1. Consequently, γ affects the maximum slope of the master curve. The three positive estimates of γ_{D1C}, γ_{D3C}, and γ_{D6C} (0.0381, 0.0386, and 0.0544, respectively) indicate that as FTC increases there is a more sudden reduction of log |E*| with f_r.

Overall Combined effect of FTC and anti-stripping agents

The top-left chart of Figure 1 shows the effects of FTC. There is an important drop of the curve with just 1 FTC. Increasing FTC from 1 to 3 causes only a slight additional reduction in log(|E*|). From 3 to 6 cycles, a larger decrease is again estimated though not as large as that obtained with the first cycle.

The top-right chart of Figure 1 shows that log(|E*|) increases for all reduced frequencies with the use of anti-stripping agents.

The middle portion of Figure 1 shows the effect of lime together with the application of 1 FTC (middle-left chart) and 6 FTC (middle-right chart). The bottom portion shows the effect of the liquid anti-strip together with the application of 1 FTC (bottom-left chart) and 6 FTC (bottom-right chart). In each case, the situation with a sample conditioned with the given number of FTC but untreated (no anti-stripping) provides a lower bound and the situation with an unconditioned sample (0 FTC) and treated with lime or liquid anti-strip provides an upper bound. The master curves for the unconditioned (0 FTC) and untreated situation (no anti-stripping) and for the conditioned (1 or 6 FTC) and treated situation (use of anti-stripping) always fall within these bounds.

Based on these results, the application of lime to a specimen conditioned with only 1 FTC is very effective at maintaining the master curve above or at the same level as the master curve for an untreated specimen without FTC. On the other hand, with 6 FTC, the application of lime is enough to restore the master curve to the level with no conditioning and no treatment but only for reduced frequencies above 10 Hz. For lower reduced frequencies, the master curve with the application of lime is still below the master curve for the unconditioned and untreated situation.

The bottom-left chart of Figure 2 shows that with 1 FTC the application of liquid anti-strip is enough to restore the master curve to the level with no conditioning and no treatment only for reduced frequencies above 0.1 Hz. However, with 6 FTC, the master curve for the liquid anti-strip treated sample is substantially below the master curve for the untreated and unconditioned situation for any reduced frequency.

CONCLUSIONS AND RECOMMENDATIONS

The following are the main conclusions:

1) Statistically significant parameter estimates were identified for the number of FTC on three of the terms of the sigmoid (ρ, α, and γ). The contribution to changes in log(|E*|) from each term varies with reduced frequency but their combination always leads to a reduction of log(|E*|) for any reduced frequency.
2) The master curves are monotonically shifted down with the number of FTC. However, these effects change with freqeeuncy.
3) The addition of hydrated lime or liquid anti-strip results in a positive vertical translation of the master curves.
4) Hydrated lime can counteract the effects of 1 FTC at any reduced frequency, but with 6 FTC, it can only do it for reduced frequencies above 10 Hz. Liquid anti-strip can counteract the effect of 1 FTC only for reduced frequencies above 0.1 Hz and, with 6 FTC, there is a net reduction of log(|E*|) at any reduced frequency.

There is a need to relate the laboratory moisture damage to field moisture damage, which would also require quantifying what the latter means. A similar approach can be used to extend this study by other states.

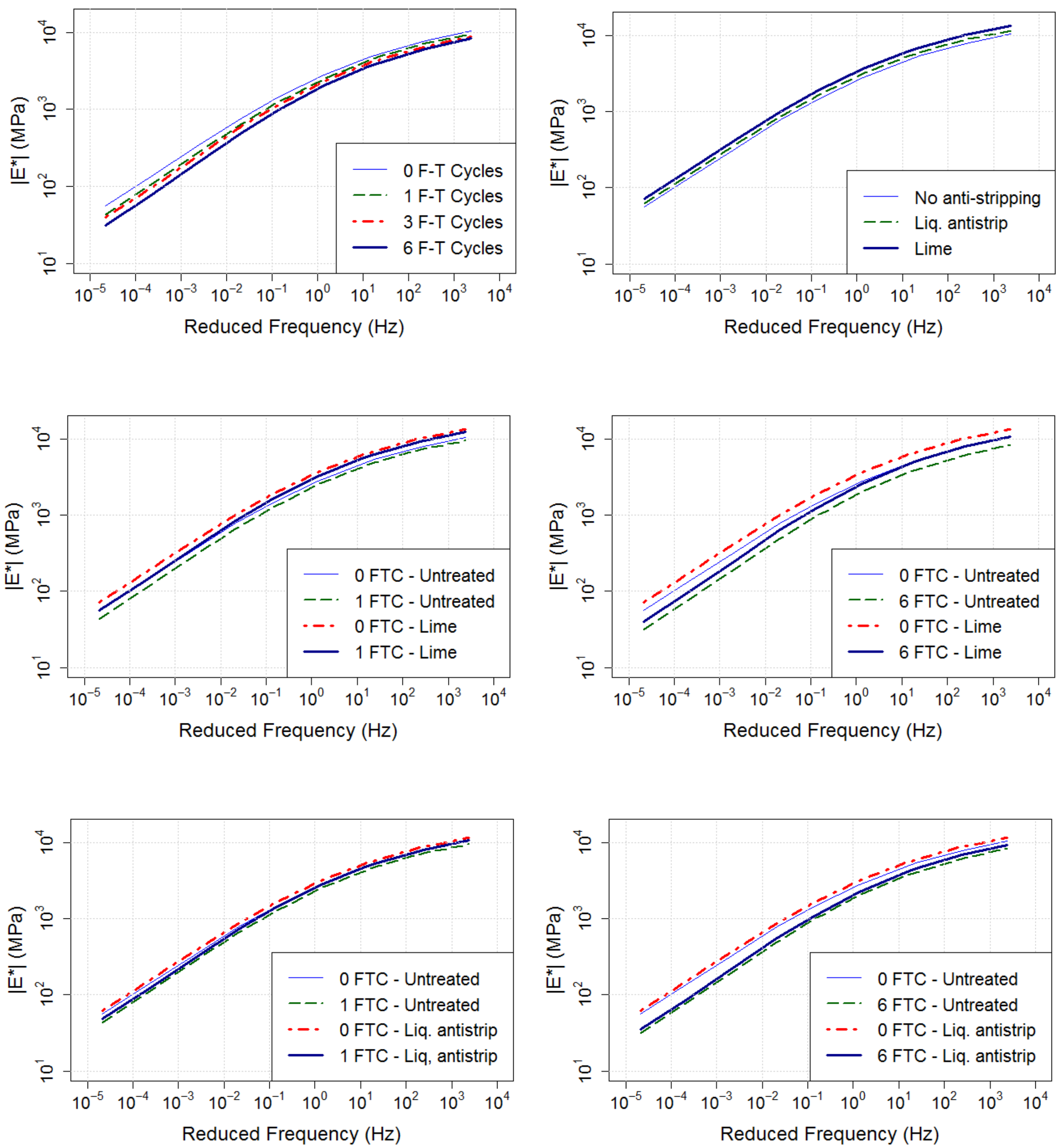

FIGURE 1 Variation of log(|E*|) solely with number of FTC (top-left); solely with anti-stripping usage (top-right); with and with without lime, with 0 and 1 FTC (middle-left); with and without lime, with 0 and 6 FTC (middle-right); with and without liquid anti-strip, with 0 and 1 FTC (bottom-left); and with and without liquid anti-strip, with 0 and 6 FTC (bottom-right) for one of the 9.5 mm NMAS specimens prepared with PMA (Specimen ID = UCR-9.5NMAS-PMA-7AV-S3).

REFERENCES

1) Corrales, J.P., A Statistical Dynamic Modulus Model of Hot Mix Asphalt using Joint Estimation and Mixed-Effects accounting for effects of confinement, moisture and additives. Ph.D. dissertation, University of Hawaii, Manoa, Honolulu, HI., 2016.
2) Kim, Y. and Lutif, J.S. *Material selection and design consideration for moisture damage of asphalt pavements.* Technical Report P564. University of Nebraska-Lincoln, Nebraska. 2006.
3) Hicks, R. *G. NCHRP Synthesis of Highway Practice 175: Moisture Damage in Asphalt Concrete*. Transportation Research Board, National Research Council, Washington, DC, 1991.
4) Hicks, R. Gray, Larry Santucci, and Tim Aschenbrener. Introduction and Seminar Objectives. In *Moisture Sensitivity of Asphalt Pavements*. CD-ROM. Transportation Research Board of the National Academies, Washington, D.C., 2004, pp. 3-20.
5) Lu, Q. and J.T. Harvey. *Investigation of Conditions for Moisture Damage in Asphalt Concrete and Appropriate Laboratory Test Methods*. Research Report No. UCPRC-RR-2005-15, University of California Pavement Research Center, UC Davis and Berkeley, 2005.
6) Little, D.N. and D.R. Jones. *Chemical and Mechanical Processes of Moisture Damage in Hot-Mix Asphalt Pavements*. In *Moisture Sensitivity of Asphalt Pavements*. CD-ROM. Transportation Research Board of the National Academies, Washington, D.C., 2004, pp. 43-74.
7) Howard, I.L., V. Gallivan and G. Huber. *Workshop Introduction*. Moisture Damage to Hot-Mix Asphalt Mixtures - Synopsis of a Workshop. Transportation Research Circular E-C198. 2012.
8) Aguiar-Moya, J.P., J. Salazar-Delgado, A. Baldi-Sevilla, F. Leiva-Villacorta, and L. Loria-Salazar. Effect of Aging on Adhesion Properties of Asphalt Mixtures with the Use of Bitumen Bond Strength and Surface Energy Measurement Tests. *Transportation Research Record: Journal of the Transportation Research Board*, No. 2505, 2015, pp. 57-65. https://doi.org/10.3141/2505-08.
9) Epps, J.A., Sebaaly, P.E., Penaranda, J., Maher, M.R., McCann, M.B. and Hand, A.J. *NCHRP Report 444*: *Compatibility of a test for moisture-induced damage with Superpave volumetric mix design.* Transportation Research Board – National Research Council. Washington, D.C. 2000.
10) Vargas-Nordcbeck, A., F. Leiva Villacorta, J.P. Aguiar Moya and L.G. Loría Salazar. Evaluating Moisture Susceptibility of Asphalt Concrete Mixtures Through Simple Performance Tests. *Transportation Research Record: Journal of the Transportation Research Board*, No. 2575, 2016, pp. 70-78. DOI: 10.3141/2575-08.
11) Solaimanian, M., J. Harvey, M. Tahmoressi, and V. Tandon. Test Methods to Predict Moisture Sensitivity of Hot-Mix Asphalt Pavements. In *Moisture Sensitivity of Asphalt Pavements*. CD-ROM. Transportation Research Board of the National Academies, Washington, D.C., 2004, pp. 77–110.
12) Hand, A. *Testing for Moisture Damage in the Laboratory*. Moisture Damage to Hot-Mix Asphalt Mixtures - Synopsis of a Workshop. Transportation Research Circular E-C198. 2012.
13) Baldi-Sevilla, A., J.P. Aguiar Moya, A. Vargas-Nordcbeck and L.G. Loría Salazar. Effect of aggregate–bitumen compatibility on moisture susceptibility of asphalt mixtures. *Road*

Materials and Pavement Design, Vol. 18, 2017, pp. 318–328. doi: 10.1080/14680629.2017.1304248.
14) Rae Hunter, E. and Ksaibati, K. (2002). *Evaluating moisture susceptibility of asphalt mixes.* Univeristy of Wyoming. Thesis Report. Laramie, Wyoming.
15) Archilla, A.R., Development of Rutting Progression Models by Combining Data from Multiple Sources. Ph.D. dissertation, University of California at Berkeley, Berkeley, CA., 2000.
16) Archilla, A.R., and Madanat, S.M., Estimation of Rutting Models by Combining data from Different Sources. *Journal of Transportation Engineering*, 2001. Volume 127(5), p. 379-389. https://doi.org/10.1061/(ASCE)0733-947X(2001)127:5(379).
17) Pinheiro, J.A., and Bates. D.M., *Mixed-Effects models in S and S-Plus*. Springer, New York, 2000.